

# Effect of frequency mismatched photons in quantum information processing

J. Metz\* and S. D. Barrett†

Blackett Laboratory, Imperial College London, Prince Consort Road, London SW7 2BW, United Kingdom

(Dated: October 28, 2018)

Many promising schemes for quantum information processing (QIP) rely on few-photon interference effects. In these proposals, the photons are treated as being indistinguishable particles. However, single photon sources are typically subject to variation from device to device. Thus the photons emitted from different sources will not be perfectly identical, and there will be some variation in their frequencies. Here, we analyse the effect of this frequency mismatch on QIP schemes. As examples, we consider the distributed QIP protocol proposed by Barrett and Kok [1], and Hong-Ou-Mandel interference which lies at the heart of many linear optical schemes for quantum computing [2, 3, 4, 5]. In the distributed QIP protocol, we find that the fidelity of entangled qubit states depends crucially on the time resolution of single photon detectors. In particular, There is no reduction in the fidelity when an ideal detector model is assumed, while reduced fidelities may be encountered when using realistic detectors with a finite response time. We obtain similar results in the case of Hong-Ou-Mandel interference – with perfect detectors, a modified version of quantum interference is seen, and the visibility of the interference pattern is reduced as the detector time resolution is reduced. Our findings indicate that problems due to frequency mismatch can be overcome, provided sufficiently fast detectors are available.

## I. INTRODUCTION

Few-photon interference effects are of fundamental interest, as they have no classical analogue, and demonstrate the quantum nature of the radiation field. The archetypal example of such an effect is two-photon interference as observed by Hong, Ou and Mandel in 1987 [6]. There two identical photons, each incident on a separate input port of a beam splitter, coalesce such that both photons are *always* detected at the same output mode of the beam splitter. More recently, single-photon interference effects have been proposed as a means to entangle remote pairs of atomic systems [7, 8]. Here, the atoms emit photons which are then incident on a beam splitter, followed by measurements on the output ports of the beam splitter. The role of the beam splitter is to coherently erase ‘*which path*’ information. Since the photons are identical and the observer cannot know which atom the photon was emitted from, the result is to prepare the pair of atoms in an entangled state.

Such interference effects are currently the subject of much interest, as they potentially provide a route to scalable quantum information processing. Few-photon interference lies at the heart of schemes for linear optics quantum computing [2, 9, 10, 11]. This is also central to many hybrid light-matter quantum computing schemes [1, 12, 13, 14], in which remote matter qubit systems (such as trapped atoms, quantum dots, or impurity centers in solids) can be entangled via single photon interference effects, in a way such that efficient quantum computation is possible. This approach can significantly simplify scaling the computer to a large number of

qubits. As a result there is now growing interest from experimental groups in implementing distributed schemes [15, 16]. Other applications of single photon interference in QIP have also been proposed, such as quantum repeaters [17, 18], and are currently being actively pursued by experimental groups [19].

Few-photon interference effects are often said to require *identical* photons, such that the frequency, polarization, and temporal envelope of each photon should be indistinguishable. This is because these experiments make use of a beam splitter to erase ‘which path’ information, so that the source of each photon cannot be inferred from the detector signal, even in principle. Any additional information carried by the photon (such as the frequency) could, in principle, be used to infer the path that the photon took, and therefore will tend to degrade the interference. From this perspective, one expects that few-photon interference cannot be observed between photons from sources of different frequency. Indeed, if one restricts ones attention to the total coincidence rates, this is indeed what is observed in a Hong-Ou-Mandel type experiments. For sufficiently detuned single photon sources, the photons behave as independent particles, each exiting either port of the beam splitter with probability  $\frac{1}{2}$ , and no interference is observed. However, this begs the question, “*where does the interference ‘go’?*” Usually we only expect quantum effects to vanish in the presence of some kind of noise or decoherence process.

Some insight into this issue has been provided in a series of intriguing theoretical and experimental results by Legero and co-workers, concerning the Hong-Ou-Mandel effect with different frequency photons [4, 5]. They showed analytically that if one can perform *time resolved* measurements in a Hong-Ou-Mandel type experiment with detuned photons, a type of quantum interference can still be observed. The probability of both photons appearing at the same output port of the beam splitter is

---

\*Electronic address: jeremy.metz@imperial.ac.uk

†Electronic address: seandbarrett@gmail.com

now no longer a constant value, but rather oscillates as a function of the time between the photon detection events. The frequency of this oscillation is given by the detuning between the two photons, and thus has been called a ‘quantum beat’ of two photons [5]. This effect was observed experimentally using successive photons from a single photon source implemented by a Raman transition in an atom-cavity system [5].

Aside from the conceptual interest in these effects, the issue of interference between photons from non-identical sources is now of significant practical importance, since there is much interest in using such effects in quantum information processing. Scaling these proposals will require observing quantum interference between photons from many different sources. These sources may be manufactured devices, such as quantum dots or other systems coupled to micro-cavities [20], and as such will be subject to fabrication imperfections. In particular, some variation of the relevant optical frequencies of the devices is to be expected. This will also be a problem in certain ‘natural’ systems, such as nitrogen-vacancy centers in diamond, which typically experience a spread in their resonance frequencies due to local strain fields [21]. While it could be possible to tune such systems over a certain frequency range, it may nevertheless be difficult to bring all of the sources into resonance with each other. Thus it is important to understand the extent to which mutual detuning of the sources induces errors in QIP schemes making use of single photon interference effects, and what can be done to mitigate such errors.

In this paper we investigate the practical and fundamental aspects of the effect of detuning on few-photon interference by considering two particular cases. Firstly, we consider the entangling operation introduced by Barrett and Kok [1]. This operation allows the preparation of entangled states of remote qubits, and furthermore can be used to generate *graph states* of multiple qubits, and hence is a resource for scalable, universal quantum computation. In addition we consider the Hong-Ou-Mandel effect. This is of interest because it is one of the best known few photon interference effects, and is also central to multiple schemes for linear optics quantum computation [2, 3] and quantum repeaters [18]. In both cases, we first consider the corresponding effects with detuned photons in the case of idealized (i.e. perfect time resolution) detectors, and find that a modified version of the entanglement/interference effect persists. We then consider the opposite case, where the detectors have very bad time resolution, and find that in this limit, the interference (or entanglement) is indeed reduced. Loosely speaking, the degree of reduction of entanglement/interference depends on the extent to which the photons are distinguishable in the frequency domain.

By making use of an explicit model of the photodetectors [22, 23], we also consider the intermediate case, where some time resolution present in the detector outputs, and quantify how the entanglement/interference is modified as the detector resolution varies. Our results

are of direct practical benefit for the implementation of these schemes, as they allow one to determine the level of error that can be expected for a given detuning and detector resolution. Furthermore, we hope the results will aid in understanding the nature of single photon interference effects with detuned photons, and give some insight into where the entanglement/interference ‘goes’.

Although we focus on two particular examples of few-photon interference in this paper, the techniques are reasonably generic and can therefore also be applied to many other schemes which involve similar effects. The effect of frequency mismatched photons has also been examined in slightly different contexts, such as sources of entangled photon pairs [24]. We also note that a potential solution to the frequency mismatch problem has been proposed [25]. This scheme makes use of acousto-optic modulators as ‘frequency beam splitters’ which can be used to erase the frequency information of the photons.

The remainder of this paper is organized as follows. In Section II we review the entangling scheme of Barrett and Kok [1]. We examine the effect of photon detuning in this scheme in Section III. The case of ideal time resolution detectors is considered in Section III A, while in III B we examine the opposite limit of very bad time resolution detectors, and in Section III C the intermediate case is analysed. In Section IV we explore the influence of detuning on the Hong-Ou-Mandel effect, again in the regimes of good, bad, and intermediate time resolution detectors. Finally, we summarize our findings and draw some conclusions in Section V.

## II. ENTANGLING ATOMS

In this section, we review the method proposed in Ref. [1] for entangling remote pairs of qubit systems, which could be trapped atoms, ions, quantum dots, or impurity centers in solids. This method actually implements a non-deterministic parity measurement such that, when successful, a projection of the form  $|01\rangle\langle 01| + |10\rangle\langle 01|$  is performed on the joint state of the qubits. A positive outcome is heralded by a particular sequence of detector clicks. If these are not observed, the operation has failed, and the qubits can be reset and the operation reattempted. This operation, combined with single qubit rotations and measurements, is sufficient to efficiently generate arbitrary graph states of multiple qubits, which in turn permit universal measurement-based quantum computation. A number of other schemes have also been proposed for remote entanglement via few-photon interference [7, 8, 12, 13, 14, 26, 27, 28, 29, 30, 31, 32], and although we do not consider these schemes explicitly, the results in this paper are expected to also be applicable to those schemes.

The setup proposed consists of two atoms [44] inside separate cavities, as shown in Figure 1, which are assumed to have equal resonant frequencies  $\omega_1 = \omega_2$ . The qubit levels  $|0\rangle$  and  $|1\rangle$  are long lived, low-lying states of

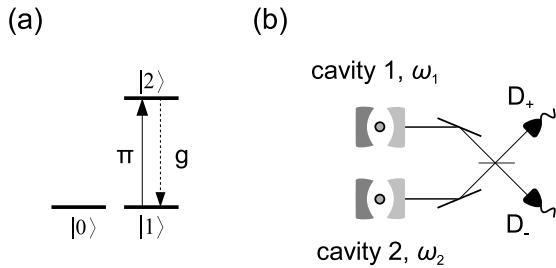


FIG. 1: Schematic diagram of the setup proposed. (a) Level structure of the atomic system.  $|0\rangle$  and  $|1\rangle$  are low lying, long lived states representing the qubit degree of freedom.  $|1\rangle$  is connected to  $|2\rangle$  by an optical transition which may be addressed by a  $\pi$ -pulse of a laser to swap population between these states, and coupled to the cavity mode with coupling constant  $g$ . (b) Setup for remote entanglement. The light from each atom is collected (possibly with the aid of an optical cavity on resonance with the  $1 \rightarrow 2$  transition) and mixed on a 50:50 beam splitter. Photon counting detectors  $D_+$  and  $D_-$  monitor the output modes of the beam splitter. In the original proposal, the frequencies  $\omega_1$  and  $\omega_2$  of the optical transitions are assumed to be equal [1]. In general, this will not be the case and we examine this scenario in Section III.

the atoms. In addition there is an excited level,  $|2\rangle$ , such that an optical transition between  $|1\rangle$  and  $|2\rangle$  couples resonantly to the cavity mode of the respective cavity. The use of cavities is not strictly necessary for the ideas presented here, since the same protocol will work if the light emitted from the optical transition is monitored in free space. However, coupling via a cavity may offer an increase in the success rate of the protocol with respect to the same setup without cavities. The protocol for entangled pair generation proceeds as follows:

1. Prepare atoms in the product state  $|+\rangle \otimes |+\rangle$ ,
2. apply a  $\pi$ -pulse on the  $2 \rightarrow 1$  transition to prepare the atoms in  $\frac{1}{2}(|00\rangle + |02\rangle + |20\rangle + |22\rangle)$ ,
3. monitor cavity output for a time significantly longer than the decay time of the  $2 \rightarrow 1$  transition; a click in either detector signals a successful first round. The absence of a click implies a failure of the operation, and the protocol should start again from step (1).
4. Apply a bit-flip,  $\sigma_x$ , on the qubit states to perform  $|0\rangle \leftrightarrow |1\rangle$  on each atom.
5. Repeat steps (2) and (3); a second click in either detector signals the successful completion of the protocol.

We now review these steps in more detail. The atoms are initially individually prepared in the  $|+\rangle \equiv \frac{1}{\sqrt{2}}(|0\rangle + |1\rangle)$  state, such that the combined state of the atoms may

be written as

$$|\psi(0)\rangle = |+\rangle \otimes |+\rangle \equiv \frac{1}{2}(|00\rangle + |01\rangle + |10\rangle + |11\rangle). \quad (1)$$

Then a  $\pi$ -pulse is applied to excite the  $1 \rightarrow 2$  transition such that the state of the atoms becomes  $\frac{1}{2}(|00\rangle + |02\rangle + |20\rangle + |22\rangle)$ . Next the cavity leakage is monitored using the detectors  $D_+$  and  $D_-$ . A click in either detector signals a successful first round of the protocol. If the detection process were perfect it would be possible to stop the protocol here and be confident of having correctly performed an entangling operation on the atoms. The final state of the atoms in this case is given by

$$|\psi^\pm\rangle = \frac{1}{\sqrt{2}}(|01\rangle \pm |10\rangle), \quad (2)$$

where the sign between the terms is determined by the detector where the click was observed. This state is obtained because the only parts of the initial state that create *exactly* one cavity excitation are initial atomic states  $|01\rangle$  and  $|10\rangle$ . The presence of the beam splitter erases the which-path information such that a click in either detector will not reveal any information about which atom/cavity the excitation originated from.

However, in general the photon collection process as well as the detectors themselves will not be perfect. Therefore the detection of a single click will lead to a mixed state over the one- and two-excitation parts of the atomic states,

$$\rho^\pm = p_1 |\psi^\pm\rangle \langle \psi^\pm| + (1 - p_1) |11\rangle \langle 11|, \quad (3)$$

where  $p_1$  is the probability of there having been only one photon. Note that strictly speaking this neglects the presence of dark counts in the detectors, which would lead to a  $|00\rangle \langle 00|$  contribution to the state. However, for existing detectors the dark count rate is typically much smaller than the atom/cavity emission rates involved in the protocol, thereby justifying this approximation. In addition, detector dead-times do not affect this protocol, since for a successful outcome, only a single click is observed on each round, and two-excitation events are rejected as a result of the post selection process (as we describe below).

The solution proposed to overcome the presence of the two-excitation component in the state, was to apply a bit-flip pulse to each qubit, i.e. a  $\sigma_x$  operation on  $|0\rangle$  and  $|1\rangle$ , followed by a second round of the protocol. The bit-flip operation has no effect on  $|\psi^\pm\rangle$ , but changes  $|11\rangle \rightarrow |00\rangle$ . Therefore a second round of the protocol resulting in a second click eliminates the  $|00\rangle$  part of the state as  $|00\rangle$  does not couple to the relevant optical fields. Thus no photon can result from this component of the state. Then the final state of the system, conditional on observing a photon in each round, is given by

$$|\psi\rangle = \frac{1}{\sqrt{2}}(|01\rangle + (-1)^m |10\rangle), \quad (4)$$

where  $m = 0$  if both clicks occur in the same detector, or  $m = 1$  if they are in different detectors. This state is maximally entangled and independent of click times. The independence on click times is due to the assumption that  $\omega_1 = \omega_2$ . We shall consider the case of detuned cavities in the following section.

The success rate of the protocol is

$$P_{\text{succ}} = \frac{1}{2}\eta^2, \quad (5)$$

where  $\eta$  is the combined efficiency of collection and detection of the photons, while the factor  $\frac{1}{2}$  is from the population of the initial state in the  $\{|01\rangle, |10\rangle\}$  subspace. In spite of the inherent non-determinism of this protocol, efficient quantum computing is still possible using this operation, in principle with any success probability larger than zero [1]. (The price to be paid for this is in an overhead cost for building the cluster states, which may become impractical for very small success probabilities [33]).

Note that the fidelity of the entangling operation is not affected by photon collection or detection efficiency, since only outcomes in which a photon was observed on each round of the protocol are retained (i.e. post-selected) as successful outcomes. This is a useful fact for analysing the fidelity of the scheme in the presence of other imperfections, since it means that one can essentially ignore the detection and collection inefficiencies in calculations, and still arrive at reliable values for the fidelity. One should still be mindful, however, that photon loss will lower the success probability. This is an approach that we will adopt in the remainder of this paper.

### III. ENTANGLING OPERATIONS WITH DETUNED SOURCES

In this section we examine the effect of cavity frequency mismatch on entangling operations. In particular we examine the scheme outlined in Section II. The setup is generalized to cavities with different frequencies,  $\omega_1$  and  $\omega_2$ . The atomic transition frequencies are each still assumed to be resonant with the corresponding cavity transition, such that  $\omega_{12;1} = \omega_1$  and  $\omega_{12;2} = \omega_2$ , where  $\omega_{12;j}$  is the frequency of the  $1 \rightarrow 2$  transition in atom  $j$ . We make this assumption partly to simplify the analysis so as to concentrate specifically on the effect of frequency mismatch *between* two sources, but it is also reasonably well motivated physically. This is because in systems where the atomic transition frequencies are not naturally on resonance with the cavity resonance, it may still be possible to tune the transitions into resonance, for example through the use of Stark or Zeeman shifts of the atomic levels. However, tuning the cavities so that they are also mutually on resonance may be more difficult, especially in the case of monolithic micro-cavities. We also restrict our attention to the case where both cavities have the same decay rate  $\kappa_1 = \kappa_2 = \kappa$ , and the same atom-cavity

coupling strength,  $g_1 = g_2 = g$ . A treatment when this is not the case has already been presented in [1].

Using the Quantum Jump (QJ) formalism [34, 35, 36, 37, 38] which is particularly well suited to describing systems under continuous observation, we find that the Hamiltonian describing the evolution of the system condition on no-photon emissions is given by

$$H_{\text{cond}}^S = \sum_{j=1}^2 \hbar\omega_j(|2\rangle_{jj}\langle 2| + b_j^\dagger b_j) + \hbar g(b_j|2\rangle_{jj}\langle 1| + b_j^\dagger|1\rangle_{jj}\langle 2|) - \frac{i\hbar\kappa}{2}b_j^\dagger b_j, \quad (6)$$

where the index  $j = 1, 2$  labels the respective atom-cavity systems. We have defined the energy of the degenerate ground states  $|0\rangle_j, |1\rangle_j$  to be zero. The first term corresponds to the energies of the atoms and the cavity fields respectively. The second term describes the Jaynes-Cummings interaction between the cavities and the 1–2 transitions of the atoms, while the last term comes from the QJ description of the cavity-free field interaction. This term is non-Hermitian and leads to a decrease in the norm of the state vector which quantifies the decrease in probability of the system not emitting photons. We now transform to an interaction picture via the unitary evolution operator  $U_0 = \exp[-\frac{i}{\hbar}\omega_1(\sum_{j=1}^2 |2\rangle_{jj}\langle 2| + b_j^\dagger b_j)t]$ . The state transforms according to  $|\psi_I(t)\rangle \equiv U_0^\dagger |\psi_S(t)\rangle$  where  $|\psi_S(t)\rangle$  is the state in the Schrödinger picture. The dynamics in the interaction picture is given by  $H_{\text{cond}}$ , where  $H_{\text{cond}} \equiv U_0^\dagger H_{\text{cond}}^S U_0 + i\hbar U_0^\dagger \dot{U}_0$ . Applying this transformation to (6) gives

$$H_{\text{cond}} = \sum_{j=1}^2 \hbar(g_j b_j |2\rangle_{jj}\langle 1| + g_j^* b_j^\dagger |1\rangle_{jj}\langle 2|) + \hbar\Delta(|2\rangle_{22}\langle 2| + b_2^\dagger b_2) - i\frac{\hbar}{2}\kappa b_j^\dagger b_j, \quad (7)$$

where we have defined  $\Delta \equiv \omega_2 - \omega_1$ . The associated jump operators which describe the evolution of the system in the event of an emission of a photon out of either cavity are given by

$$\begin{aligned} R_1 &= \sqrt{\kappa} b_1, \\ R_2 &= \sqrt{\kappa} b_2. \end{aligned} \quad (8)$$

Now the *unconditional* master equation for this dissipative system may be written as

$$\dot{\rho} = \frac{i}{\hbar}(H_{\text{cond}}\rho - \rho H_{\text{cond}}^\dagger) + R_1\rho R_1^\dagger + R_2\rho R_2^\dagger. \quad (9)$$

The effect of a 50-50 beam splitter which mixes the cavity outputs  $b_1$  and  $b_2$ , as described in Section II is described by the beam splitter transformation,

$$\begin{aligned} c_+ &= \frac{b_1 + b_2}{\sqrt{2}}, \\ c_- &= \frac{b_1 - b_2}{\sqrt{2}}, \end{aligned} \quad (10)$$

where  $c_+$  and  $c_-$  are the two output modes of the beam splitter. Note that the transformed operators,  $c_+$  and  $c_-$ , do not have an explicit time dependence in the interaction picture. This is a consequence of the form of  $U_0$  – both cavity jump operators,  $b_{1,2}$ , receive the same time-dependent phase shift, and so there is no relative phase between the  $b_1$  and  $b_2$  terms in the transformation. This transformation leaves the master equation unchanged, but will however influence single trajectories. This is reflected by the change in jump operators,

$$\begin{aligned} R_+ &= \sqrt{\frac{\kappa}{2}}(b_1 + b_2) = \sqrt{\kappa}c_+, \\ R_- &= \sqrt{\frac{\kappa}{2}}(b_1 - b_2) = \sqrt{\kappa}c_-. \end{aligned} \quad (11)$$

Now we use the fact that for the over damped (i.e. Purcell) regime, i.e. when  $\kappa \gg g$ , we may eliminate the populated cavity mode to simplify the analysis [39]. This approximation is possible as the population in the cavity mode remains negligible in this regime. Then we find that the effective Hamiltonian of the system is then given by

$$H_{\text{cond}} = \hbar\Delta|2\rangle_{22}\langle 2| - \sum_{j=1}^2 i\frac{\hbar}{2}\kappa_{\text{eff}}|2\rangle_{jj}\langle 2|, \quad (12)$$

where  $\kappa_{\text{eff}} \equiv 4g^2/\kappa$  is the effective decay rate of the atoms, for decay via the cavity mode. Similarly the effective jump operators are given by

$$\begin{aligned} R_+ &= \sqrt{\frac{\kappa_{\text{eff}}}{2}}(|1\rangle_{11}\langle 2| + |1\rangle_{22}\langle 2|), \\ R_- &= \sqrt{\frac{\kappa_{\text{eff}}}{2}}(|1\rangle_{11}\langle 2| - |1\rangle_{22}\langle 2|). \end{aligned} \quad (13)$$

Note that Eqs. (12–13) are also applicable to setups with no cavities, where the spontaneously emitted light is directly collected via a system of lenses and other optical elements [15, 16]. In this case,  $\kappa_{\text{eff}}$  should be replaced by the appropriate rate for spontaneous emission into the collected mode.

### A. Ideal detector case

In this section we consider the case of remote entangling operations in the case where the time resolution of the detectors,  $t_r$ , is ‘ideal’, in the sense that it is very much shorter than  $1/\Delta$ . The time resolution can be understood as the uncertainty in the time at which the photon caused a change in the detector, due to technical imperfections in the detector, and finite bandwidth of the associated electronics. Note that we cannot assume truly infinitesimal time resolution, since the quantum jumps formalism that we apply here uses Born, Markov, and rotating wave approximations which break down on very

short timescales on the order of the inverse of the optical frequency. Thus the results in this section are valid in the regime  $1/\omega_{1,2} \ll t_r \ll 1/\Delta$ .

As noted at the end of Section II, we can analyze the scheme as if the collection and detection efficiency was perfect, since we are only interested in the final state in the case when detector clicks were actually observed on both rounds of the protocol. Finite collection and detection efficiencies will not affect this conditional state, but will simply reduce the overall success probability. In this case, the evolution of the system when no detector clicks are observed is described by the Schrödinger equation,

$$\frac{d}{dt}|\psi(t)\rangle = -\frac{i}{\hbar}H_{\text{cond}}|\psi(t)\rangle. \quad (14)$$

Since  $H_{\text{cond}}$  is non-Hermitian, this evolution is non-unitary, and thus  $|\psi(t)\rangle$  is unnormalized. The norm-squared of the wavefunction,  $|\psi(t)\rangle^2$ , can be interpreted as the probability that the system has not emitted any photons since the previous emission event.

In the event of a detector click in the  $D_+$  or  $D_-$  detectors, the state evolves discontinuously according to

$$\begin{aligned} |\psi'_+\rangle &= \frac{R_+|\psi\rangle}{\langle\psi|R_+^\dagger R_+|\psi\rangle}, \\ |\psi'_-\rangle &= \frac{R_-|\psi\rangle}{\langle\psi|R_-^\dagger R_-|\psi\rangle}, \end{aligned} \quad (15)$$

respectively. The corresponding probability density for a click in either detector is given by

$$u(t, \pm) = \langle\psi(t)|R_\pm^\dagger R_\pm|\psi(t)\rangle. \quad (16)$$

Here,  $u(t, \pm)dt$  is the total probability that a click occurs in detector  $D_\pm$  between times  $t$  and  $t + dt$ , and that no click occurred before time  $t$ .

Following the first optical  $\pi$ -pulse, the state of the two-atom system at  $t = 0$  is given by  $|\psi(0)\rangle = \frac{1}{2}(|00\rangle + |02\rangle + |20\rangle + |22\rangle)$ . Note that we are interested only in the parts of the state that will ultimately be post-selected conditional on observing detector clicks on both rounds of the protocol. Thus we can restrict attention to the components of the state in the subspace spanned by the states  $|01\rangle$ ,  $|10\rangle$ ,  $|02\rangle$ , and  $|20\rangle$ . This leads to the following closed set of coupled equations for the evolution generated by Eq. (14),

$$\begin{aligned} \dot{c}_{02} &= -i\Delta c_{02} - \frac{\kappa_{\text{eff}}}{2}c_{02}, \\ \dot{c}_{20} &= -\frac{\kappa_{\text{eff}}}{2}c_{20}, \\ \dot{c}_{01} &= 0, \\ \dot{c}_{10} &= 0, \end{aligned} \quad (17)$$

where  $c_{jk}(t) = \langle j|k|\psi(t)\rangle$ . Eqs. (17) may be readily solved to give

$$\begin{aligned} c_{02}(t) &= c_{02}(0)e^{-(i\Delta + \kappa_{\text{eff}}/2)t}, \\ c_{20}(t) &= c_{20}(0)e^{-\kappa_{\text{eff}}t/2}. \end{aligned} \quad (18)$$

Since  $c_{02;00}(0) = c_{20;00}(0)$ , we see that these two coefficients are identical up to a varying phase factor,

$$c_{02} = e^{-i\Delta t} c_{20}. \quad (19)$$

By applying Eq. (15), we find that the normalized zero-excitation component of the state after the first click at  $t_1$  is given by

$$|\psi_{\pm}(t_1)\rangle = \frac{|01\rangle \pm e^{i\Delta t_1} |10\rangle}{\sqrt{2}}, \quad (20)$$

corresponding to a click in the  $D_+$  or  $D_-$  detector respectively. Note that the true state will include terms proportional to  $|12\rangle$  and  $|21\rangle$ . However, these will be post-selected away on the second round of the protocol, and so can be neglected for the purposes of this analysis. Proceeding with the second round as described in Section II, we find that the second click at  $t_2$  removes these unwanted terms, and leaves the system in

$$|\psi(t_1, t_2)\rangle = \frac{|01\rangle + (-1)^m e^{i\Delta(t_1-t_2)} |10\rangle}{\sqrt{2}}, \quad (21)$$

where  $m$  is the number of  $D_-$  clicks that have been observed. We note that regardless of the actual values of  $t_1$  and  $t_2$ , the final state for any detector click combination is always a maximally entangled state. In addition, as long as the values  $t_1$  and  $t_2$  are known, it is possible in principle to undo this additional phase shift in the system with a local operation. This may be achieved via a rotation about the  $z$ -axis by an angle  $-\Delta(t_1 - t_2)$  on the first qubit. Therefore in this ideal case the fidelity of the protocol is unity despite mismatch of the cavity frequencies.

This result can be understood as follows. In general we might expect a reduction in fidelity due to the fact that the frequency of the photons carries some ‘which path’ information about which of the atoms the detected photons originated from. However, since we have assumed idealized time-resolution detectors, complementary information about the frequency of the photon cannot be determined, even in principle. Thus these idealized detectors themselves erase the ‘which path’ information, contained in the frequencies of the photons, which might otherwise have reduced the fidelity.

## B. Bad detector limit

We now consider the case of very bad time resolution detectors, when  $t_r \gg \Delta^{-1}$ ,  $\kappa_{\text{eff}}^{-1}$ . In this regime, the detectors give essentially no information about the arrival time of the photons, but simply indicate whether a photon was observed or not on a given round of the protocol. We again assume that the collection and detection efficiencies are unity.

By inspecting Eq. (21) it is clear that, since  $t_1$  and  $t_2$  will now be unknown, an unknown phase will be accumulated between the two terms in the superposition.

Averaging over this phase will lead to a mixed state, with less than ideal fidelity. Assuming the click is observed in detector  $D_+$ , the state at the end of the first round of the protocol will be

$$\begin{aligned} \bar{\rho}_+ &= \frac{1}{p(+)} \int_0^\infty dt_1 p(t_1, +) \\ &\times \frac{1}{2} (|10\rangle + e^{-i\Delta t_1} |01\rangle) (\langle 10| + e^{i\Delta t_1} \langle 01|). \end{aligned} \quad (22)$$

Here,  $p(t_1, +)dt$  is the probability that a single photon is emitted into  $D_+$  between times  $t_1$  and  $t_1 + dt$ , and that no photon is observed subsequently in either detector.  $p(+)$  is the total probability of observing precisely one photon in  $D_+$ , and no photons in  $D_-$ . These quantities can be calculated within the QJ method to give

$$p(t_1, +) = \frac{\kappa_{\text{eff}} e^{-\kappa_{\text{eff}} t_1}}{4}, \quad (23)$$

from which we obtain  $p(+)$  is  $1/4$ . The state of the system at the end of the first round is found to be

$$\begin{aligned} \bar{\rho}_+ &= \frac{1}{2} (|01\rangle\langle 01| + |10\rangle\langle 10| \\ &+ \frac{\kappa_{\text{eff}}}{\kappa_{\text{eff}} + i\Delta} |01\rangle\langle 10| + \frac{\kappa_{\text{eff}}}{\kappa_{\text{eff}} - i\Delta} |10\rangle\langle 01|). \end{aligned} \quad (24)$$

To determine the effect of the second round of the protocol, we use  $\bar{\rho}_+$  as the input, and evolve under the generalized Schrödinger equation,  $\dot{\rho}(t_2) = -\frac{i}{\hbar} [H_{\text{cond}} \rho(t_2) - \rho(t_2) H_{\text{cond}}^\dagger]$ . The state corresponding to a click in  $D_+$  at time  $t_2$  is then  $R_+ \bar{\rho}_+(t_2) R_+^\dagger / \text{tr}[R_+ \bar{\rho}_+(t_2) R_+^\dagger]$ , and the corresponding probability density is  $p(t_2, +) = \text{tr}[R_+ \bar{\rho}_+(t_2) R_+^\dagger]$ . From this we find that the final state, after both rounds of the protocol, is given by

$$\begin{aligned} \bar{\rho}_{++} &= \int_0^\infty dt_2 R_+ \bar{\rho}_+(t_2) R_+^\dagger, \\ &= \frac{1}{2} (|01\rangle\langle 01| + |10\rangle\langle 10| \\ &+ \frac{\kappa_{\text{eff}}^2}{\kappa_{\text{eff}}^2 + \Delta^2} (|01\rangle\langle 10| + |10\rangle\langle 01|)). \end{aligned} \quad (25)$$

A useful figure of merit for evaluating the effect of frequency mismatch is the fidelity of the final state with the closest maximally entangled state. Note that the protocol is such that the final state only has components in the  $\{|01\rangle, |10\rangle\}$  basis, so the closest maximally entangled state will be of the form  $|\psi(\phi)\rangle = (|01\rangle + e^{i\phi} |10\rangle) / \sqrt{2}$ . Thus, for a given state  $\rho$ , the fidelity can be found by maximizing

$$F(\rho, \phi) = \langle \psi(\phi) | \rho | \psi(\phi) \rangle, \quad (26)$$

with respect to  $\phi$ , i.e. solving  $\partial F(\rho, \phi) / \partial \phi = 0$ . Doing so we find that  $\phi = -\arg(\rho_{01,10})$ , and that the fidelity is given by

$$F(\rho) = \frac{1}{2} + |\rho_{01,10}|. \quad (27)$$

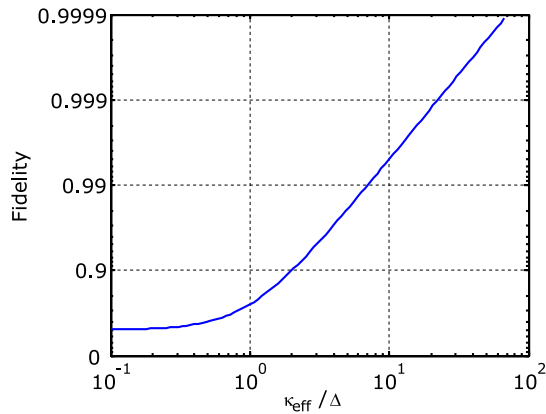


FIG. 2: Log-log plot of the final state fidelity as a function of  $\kappa_{\text{eff}}/\Delta$ . We notice that even for a bad detector which is in principle able to distinguish the different frequency photons, a very high fidelity is possible provided that the bandwidth of the photons is large compared with their detuning.

Substituting  $\bar{\rho}_{++}$  from Eq. (25) gives

$$F(\bar{\rho}_{++}) = \frac{1}{2} \left( 1 + \frac{\kappa_{\text{eff}}^2}{\kappa_{\text{eff}}^2 + \Delta^2} \right). \quad (28)$$

We plot this result in Figure 2.  $F(\bar{\rho}_{++})$  increases toward unity for  $\kappa_{\text{eff}} \gg \Delta$ . This result can be understood by considering the spectrum of the emitted photons. More specifically,  $\kappa_{\text{eff}}$  can be thought of as the bandwidth of each photon in the frequency domain. Thus for  $\kappa_{\text{eff}} \gg \Delta$ , the photons become spectrally indistinguishable, and therefore carry no which-path information. In this regime we can obtain a large fidelity, even with very low time-resolution detectors.

### C. Intermediate detector case

In this section we describe the effect of having a detector with arbitrary time resolution, which may lie between the two limiting cases already studied in the preceding sections. This requires a more sophisticated model of the detection process to include a finite time resolution.

The detector model we use is similar to the one described in Refs. [22, 23], and is summarized in Figure 3. While the complete model in Refs. [22, 23] incorporates a number of realistic imperfections, including finite time resolution, dead time, and dark counts, here we restrict our attention to the effect of finite time resolution alone.

We now briefly review the model of [22, 23] for the case of a single fluorescing quantum system, observed by a single detector, neglecting dead time and dark counts. In this case [22, 23], the model consists of an idealized detector coupled to the transition between two internal states, *ready* and *triggered* (denoted here by  $R$  and  $T$ , respectively), of the detector. When a photon is registered by the ideal detector, the internal state changes from  $R$

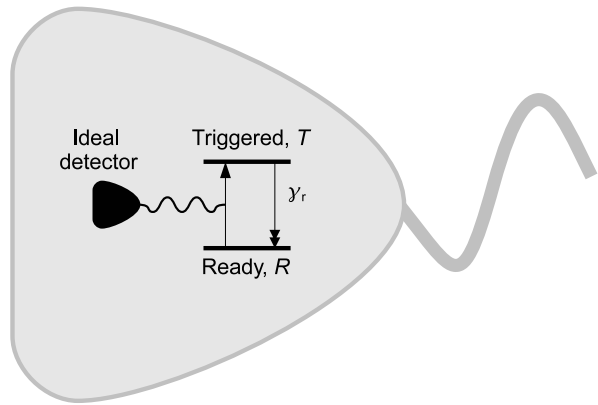


FIG. 3: Diagram showing the detector model adopted here to take account of the finite time resolution of the detector.

to  $T$ . The  $T$  state of the detector decays, via a Poisson process, back to  $R$  at a rate  $\gamma_r$ . This decay process can be understood as the observed detector ‘click’, i.e. the time of the  $T \rightarrow R$  transition corresponds to the photon detection time reported to the observer.  $\gamma_r^{-1}$  can be understood as the response time of the detector.

The quantities of interest are the unnormalized density matrices  $\rho_R(t)$  and  $\rho_T(t)$ .  $\rho_R(t)$  corresponds to the state of the quantum system at time  $t$ , given that the detector is in the ‘ready’ state, while  $\rho_T(t)$  corresponds to the state of the quantum system given that the detector is in the ‘triggered’ state. The states are unnormalized, such that  $\text{tr}[\rho_R(t) + \rho_T(t)]$  is the total probability that no click has been observed up to time  $t$  (provided the state was normalized at time  $t = 0$ ). The normalized state of the system at arbitrary times is then given by  $\rho(t) = [\rho_R(t) + \rho_T(t)]/\text{tr}[\rho_R(t) + \rho_T(t)]$ .

Between detector clicks, the state evolves according to the generalized master equation

$$\begin{aligned} \dot{\rho}_R &= (\mathcal{L} - J[R])\rho_R, \\ \dot{\rho}_T &= (\mathcal{L} - \gamma_r)\rho_T + J[R]\rho_R, \end{aligned} \quad (29)$$

where  $\mathcal{L}\rho \equiv -\frac{i}{\hbar}(H_{\text{cond}}\rho - \rho H_{\text{cond}}^\dagger) + R\rho R^\dagger$  is the usual Lindblad superoperator, and  $J[R]\rho \equiv R\rho R^\dagger$  is the jump superoperator.  $R$  here is the appropriate lowering operator for the fluorescing system of interest, with  $H_{\text{cond}}$  the corresponding conditional, non-Hermitian Hamiltonian.

The first equation corresponds to the conditional evolution for the case when no photon is emitted, and is a generalization of Eq. (14) to mixed states. The second equation has three contributions. The term  $\mathcal{L}\rho_T$  corresponds to the unconditional evolution of the system, i.e. it is what would be expected if there were no detector present. This can be understood since, once the detector is in the triggered state, no more information about the state of the system can be obtained from the detector until it returns to the ‘ready’ state via a ‘click’ event. The term proportional to  $\gamma_r\rho_T$  ensures that  $\rho_T$  is appropriately normalized, given that no click has been observed.

Finally, the  $J[R]\rho_R$  term couples the two equations and corresponds to  $R$  to  $T$  transitions of the detector when a photon is received.

The probability distribution for observing a detector click at time  $t$ , given that no clicks were observed until time  $t$ , and provided the state was normalized at time  $t = 0$ , is given by

$$p(t) = \gamma_r \text{tr}[\rho_T(t)]. \quad (30)$$

When a click occurs, the state evolves discontinuously as

$$\begin{aligned} \rho_R(t+dt) &= \rho_T(t), \\ \rho_T(t+dt) &= 0. \end{aligned} \quad (31)$$

Eqs. (29–31) allow one to calculate the probability distributions for click times, and also to determine the state of the system at arbitrary times, conditional on the record of detector click times.

It is straightforward to generalize this model to the case of two detectors, observing two atoms via a beam splitter. We now have to track four quantities,  $\rho_{RR}$ ,  $\rho_+$ ,  $\rho_-$ , and  $\rho_{TT}$ .  $\rho_{RR}$  corresponds to the state of the two atom system when both detectors are in the ready state.  $\rho_+$  ( $\rho_-$ ) corresponds to the detector  $D_+$  in the triggered (ready) state, and  $D_-$  in the ready (triggered) state.  $\rho_{TT}$  corresponds to both detectors being in the triggered state.

The set of equations governing the evolution of the system conditioned on *no detector click* is

$$\begin{aligned} \dot{\rho}_{RR} &= (\mathcal{L} - J[R_+] - J[R_-])\rho_{RR}, \\ \dot{\rho}_+ &= (\mathcal{L} - J[R_-] - \gamma_r)\rho_+ + J[R_+]\rho_{RR}, \\ \dot{\rho}_- &= (\mathcal{L} - J[R_+] - \gamma_r)\rho_- + J[R_-]\rho_{RR}, \\ \dot{\rho}_{TT} &= (\mathcal{L} - 2\gamma_r)\rho_{++} + J[R_-]\rho_+ + J[R_+]\rho_-, \end{aligned} \quad (32)$$

where  $\mathcal{L}\rho \equiv -\frac{i}{\hbar}(H_{\text{cond}}\rho - \rho H_{\text{cond}}^\dagger) + R_+\rho R_+^\dagger + R_-\rho R_-^\dagger$  is the Lindblad master equation,  $J[R]\rho \equiv R\rho R^\dagger$  is the jump matrix, and  $\gamma_r$  is the stochastic decay rate at which a triggered detector will signal a click and return into the ready state.

The complimentary (instantaneous) evolution corresponding to a  $D_+$  click event is now

$$\begin{aligned} \rho_{RR}(t+dt) &= \rho_+(t), \\ \rho_+(t+dt) &= 0, \\ \rho_-(t+dt) &= \rho_{TT}(t), \\ \rho_{TT}(t) &= 0. \end{aligned} \quad (33)$$

while a  $D_-$  click event is described by

$$\begin{aligned} \rho_{RR}(t+dt) &= \rho_-(t), \\ \rho_+(t+dt) &= \rho_{TT}(t), \\ \rho_-(t+dt) &= 0, \\ \rho_{TT}(t) &= 0. \end{aligned} \quad (34)$$

We may solve the coupled equations of (32) analytically in the over damped regime, where  $H_{\text{cond}}$  and  $R_\pm$  are given by Eqs. (12 - 13). The analysis can be considerably simplified by noting that we are only interested in the case where a single detector click is observed on each round of the protocol, since other outcomes will be discarded as failures anyway. This means that we need only to explicitly keep track of terms in the state which contain a single excitation.

Evaluating the Eqs. (32–34), for the case when exactly one detector click is observed on each round of the protocol, leads to the final state of the system given by

---


$$\begin{aligned} \rho_{01,01}(t_1, t_2) &= \frac{\rho_{20,20;0}(0)\kappa_{\text{eff}}^2}{4(\kappa_{\text{eff}} - \gamma_r)^2} e^{-\gamma_r(t_1+t_2)} (e^{-(\kappa_{\text{eff}}-\gamma_r)t_1} - 1)(e^{-(\kappa_{\text{eff}}-\gamma_r)t_2} - 1), \\ \rho_{01,10}(t_1, t_2) &= \frac{(-1)^m \rho_{20,02;0}(0)\kappa_{\text{eff}}^2}{4(i\Delta + \kappa_{\text{eff}} - \gamma_r)^2} e^{-\gamma_r(t_1+t_2)} (e^{-(i\Delta+\kappa_{\text{eff}}-\gamma_r)t_1} - 1)(e^{-(i\Delta+\kappa_{\text{eff}}-\gamma_r)t_2} - 1), \\ \rho_{10,10}(t_1, t_2) &= \frac{\rho_{02,02;0}(0)\kappa_{\text{eff}}^2}{4(\kappa_{\text{eff}} - \gamma_r)^2} e^{-\gamma_r(t_1+t_2)} (e^{-(\kappa_{\text{eff}}-\gamma_r)t_1} - 1)(e^{-(\kappa_{\text{eff}}-\gamma_r)t_2} - 1), \end{aligned} \quad (35)$$


---

where  $t_1$  and  $t_2$  are the times of the observed detector clicks on the corresponding rounds of the protocol, and  $m = 0$  if both clicks are in the same detector, else  $m = 1$ . All other components of the density matrix vanish. Note that, as before, this state is unnormalized, with the normalization such that the joint probability distribution for any specific two click combination is given by  $P(t_1, t_2) \equiv \gamma_r^2 \text{tr}[\rho(t_1, t_2)]$ . As expected, this expression integrates to  $\frac{1}{8}$  which is the total probability of having

exactly two clicks in a specific sequence such as  $D_+$  followed by  $D_+$ .

For  $\Delta \gg \kappa_{\text{eff}}, \gamma_r$  we see that the coherence vanishes corresponding to a large amount of mixing, which confirms the results from Section III B. Similarly, for  $\Delta \ll \kappa_{\text{eff}}, \gamma_r$ , we find that we recover the pure, maximally entangled state from Section III A.

More specifically, using Eq. (27) we find that the fidelity of the protocol for this intermediate detector case

is given by

$$F(t_1, t_2) = \frac{1}{2} + 0.5 \frac{(\kappa - \gamma_r)^2}{(\kappa - \gamma_r)^2 + \Delta^2} \frac{|(e^{-(i\Delta + \kappa - \gamma_r)t_1} - 1)(e^{-(i\Delta + \kappa - \gamma_r)t_2} - 1)|}{(e^{-(\kappa - \gamma_r)t_1} - 1)(e^{-(\kappa - \gamma_r)t_2} - 1)}. \quad (36)$$

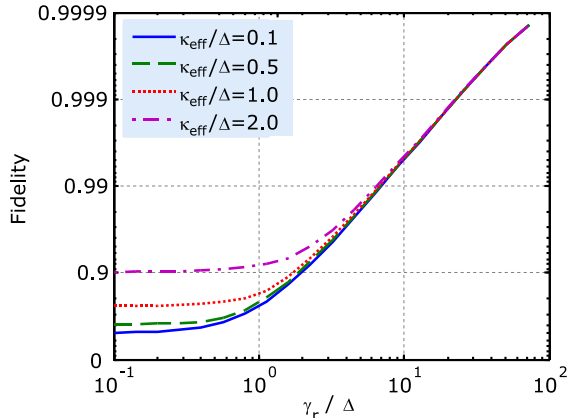


FIG. 4: (Colour online) Average final fidelity for the intermediate detector regime, from a numerical evaluation of Eq. (38).

The average fidelity of the protocol is then

$$\bar{F} = \frac{\int_0^\infty dt_1 \int_0^\infty dt_2 P(t_1, t_2) \cdot F(t_1, t_2)}{\int_0^\infty dt_1 \int_0^\infty dt_2 P(t_1, t_2)}. \quad (37)$$

Using Eqs. (35) and (27) and the joint probability density for the clicks,  $P(t_1, t_2)$ , this simplifies to

$$\bar{F} = \frac{1}{2} + \int_0^\infty dt_1 \int_0^\infty dt_2 8\gamma_r^2 |\rho_{01,10}(t_1, t_2)|. \quad (38)$$

This expression is not readily integrable analytically, but it may be solved numerically. Doing so for a range of  $\gamma_r$  and  $\kappa_{\text{eff}}$  gives the results plotted in Figures 4 and 5. Figure 4 indicates that the error in the entangling operation [that is,  $1 - \bar{F}$ , with  $\bar{F}$  the average fidelity of Eq. (38)] scales approximately quadratically with  $\Delta/\gamma_r$ , and also indicates that for fidelities exceeding 0.99 we require  $\gamma_r \gtrsim 6\Delta$ . We also find that  $\kappa_{\text{eff}}$  and  $\gamma_r$  have similar influences on the final state fidelity, as can be seen from the plot shown in Figure 5.

#### IV. HONG-OU-MANDEL DIP WITH DETUNED SOURCES

In this section, we consider another few-photon interference phenomenon, the Hong-Ou-Mandel (HOM) effect, with detuned photons. The HOM effect is well understood and was first observed in 1987 [6]. In the usual

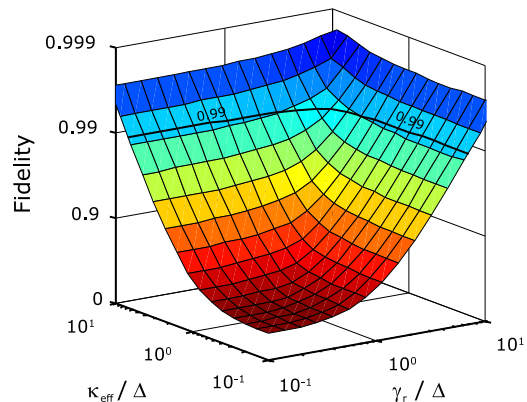


FIG. 5: (Colour online) Average final fidelity for the intermediate detector regime, from a numerical evaluation of Eq. (38), as a function of both  $\kappa_{\text{eff}}$  and  $\gamma_r$ .

setup, two photons with identical spectra and spatio-temporal mode shapes simultaneously impinge on the two different input ports of a beam splitter. Provided these photons are identical and phase coherent, the state at the output ports of the beam splitter is then given by  $|\psi_{\text{out}}\rangle = (|2, 0\rangle + |0, 2\rangle)/\sqrt{2}$ . In this idealized situation, subsequent detection of the photons by photodetectors placed at each output port thus reveals perfect *bunching* or *coalescence* of the photons; that is, both detection events occur in the same detector, and coincidences corresponding to one photon leaving each output port of the beam splitter are not detected.

The HOM effect was originally used to characterize the coherence of individual photons from parametric down conversion sources [6], and has also been used to characterize photons from a single quantum dot source [40]. More recently, this effect has been used as the basis of many schemes for linear optical quantum computing [2, 3], and has been proposed as a method for entangling spatially separated atomic ensembles [18]. The effect has recently been observed using photons from independent sources, such as independently trapped neutral atoms [41] and separate ions [42].

The ubiquity and utility of this phenomenon in quantum information processing therefore motivates the quantitative study of the HOM effect when the photons are not identical, in particular when the center frequency of the two photons is not identical. HOM interference of such detuned photons has already been studied both the-

oretically [4] and in an elegant experiment using photons from an atom-cavity system [5]. Legero *et al.* predicted, and subsequently observed, that perfect photon coalescence is not seen. Rather, provided sufficient time resolution is available in the detector signals, the probability of detecting both photons in the same detector oscillates as a function of the detection time, with the frequency of this beat oscillation given by the relative detuning of the two input photons.

Here, we study this effect using a similar method to that described in Section III, i.e. we treat the effect as a continuous measurement problem, and keep track of the internal quantum state of the sources. In Section IV A we consider the limit of ideal detectors, namely ones for which precise information about the timing of the detection events is available. As noted above, a similar calculation has already been performed in [4] using different techniques. We obtain results in agreement with Ref. [4], which demonstrates the validity of our approach, and furthermore, we hope sheds an alternative perspective on the result. Then in Section IV B we discuss the opposite limit, and determine the coalescence probability in the case where no timing information is available from the detectors. We quantitatively consider the intermediate case in Section IV C, where the detectors have finite time resolution, and evaluate the visibility of the HOM beat fringes as a function of the both the photon detuning and detector resolution.

### A. Ideal detector case

In this section we consider the HOM effect with detuned photons, of center frequencies  $\omega_1$  and  $\omega_2 = \omega_1 - \Delta$  in the limit of detectors with time resolution much shorter than  $\Delta^{-1}$ . We use a simple model of the single photon sources, comprising single mode leaky cavities, each initially prepared in the single photon Fock state, as shown in Figure 6.

As elsewhere in this paper, we treat this setup as a continuous measurement experiment, and apply the QJ formalism. We assume, for simplicity, that the efficiencies for photodetection, collection, and photon emission into the desired mode are all unity. This assumption can be relaxed later. Provided the emission efficiencies are identical, the results will be essentially the same, except for an overall reduction in coincidence count rate.

The quantities of interest are the time-resolved coincidence probability density functions,  $p(t_1, t_2, \pm, \pm)$ . For instance,  $p(t_1, t_2, +, -)dt_1dt_2$  is the probability that the first click is observed in the detector  $D_+$  in the infinitesimal interval  $[t_1, t_1 + dt_1]$ , and that the second click is observed in  $D_-$  in the interval  $[t_2, t_2 + dt_2]$ . We restrict our attention here to the quantity  $p(t_1, t_2, +, +)$ , but the other quantities are straightforward to calculate in a similar manner (in particular the symmetry of the setup implies  $p(t_1, t_2, +, +) = p(t_1, t_2, -, -)$ ).

Between photodetection events, i.e. conditional on no

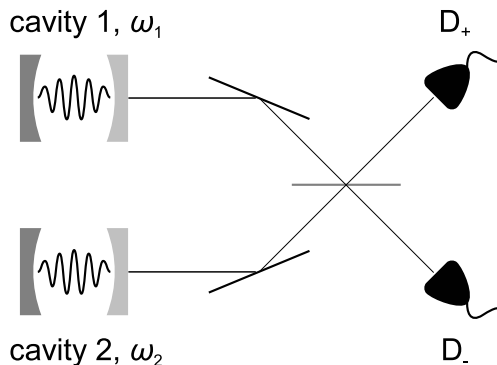


FIG. 6: (Colour online) Set-up for a HOM experiment with detuned photons. The single photon sources are each modeled as single mode cavities, with a leaky mirror of decay rate  $\kappa$  at one end. The frequencies of the cavities (and hence the emitted photons) are  $\omega_1$  and  $\omega_2 = \omega_1 - \Delta$  respectively. The sources are initially prepared in the single photon Fock state  $|1, 1\rangle = c_1^\dagger c_2^\dagger |0, 0\rangle$ . Photons emitted from these sources impinge on the two different input ports of a beam splitter, and are subsequently detected by the photodetectors  $D_+$  and  $D_-$ . The cavity sources may be replaced with a variety of different physical systems, with qualitatively similar results, as described in the text.

detector clicks, the cavity systems evolve under the Schrödinger equation [Eq. (14)] according to the non-Hermitian conditional Hamiltonian

$$H_{\text{cond}} = \hbar\omega_1 b_1^\dagger b_1 + \hbar\omega_2 b_2^\dagger b_2 - \frac{i\hbar\kappa}{2} b_1^\dagger b_1 - \frac{i\hbar\kappa}{2} b_2^\dagger b_2. \quad (39)$$

Here,  $\omega_j$  is the frequency of cavity  $j$  (and hence the central frequency of the emitted photon),  $b_j$  are the corresponding lowering operators, and  $\kappa$  is the leakage rate of each cavity. For simplicity, we assume that the cavity leakage rate, and hence the temporal mode shape of the emitted photons, is the same for each cavity.

As in Section III, in the event of a detection event the system evolves discontinuously according to

$$|\psi'_+\rangle = \frac{R_+|\psi\rangle}{\langle\psi|R_+^\dagger R_+|\psi\rangle}, \quad (40)$$

$$|\psi'_-\rangle = \frac{R_-|\psi\rangle}{\langle\psi|R_-^\dagger R_-|\psi\rangle}. \quad (41)$$

In this case, the jump operators are given directly by the beam splitter transformation,

$$R_+ = \sqrt{\frac{\kappa}{2}}(b_1 + b_2), \\ R_- = \sqrt{\frac{\kappa}{2}}(b_1 - b_2). \quad (42)$$

It is worth noting that while Eqs. (39) and (42), together with the initial condition that each cavity is prepared in a Fock state, represent a rather idealized model

of a single photon source, they are also directly relevant for more realistic systems that could be used as sources. These include isolated two-level atomic systems (such as trapped atoms, ions, quantum dots, impurity centers in diamond), or corresponding systems coupled to a single (adiabatically eliminated) cavity mode in the bad-cavity regime. In such cases, the cavity mode is replaced with the corresponding atomic transition, and the lowering operators  $b_j$  should be replaced with the corresponding lowering operator for the atomic system, similarly to Section III. The results below therefore also apply to these alternative systems.

We assume the cavities are initially prepared in the Fock state  $|\psi(0)\rangle = |1, 1\rangle = b_1^\dagger b_2^\dagger |0, 0\rangle$ , where  $|0, 0\rangle$  represents the vacuum mode for both cavities. Subsequently, conditioned on no detector clicks being observed between times 0 and  $t_1$ , the state for the cavities evolves according to  $|\tilde{\psi}(t_1)\rangle = \exp(-\frac{i}{\hbar} H_{\text{cond}} t_1) |\psi(0)\rangle = \exp[-(i\omega_1 + i\omega_2 + \kappa)t_1] |1, 1\rangle$ .

Assuming a click occurs at time  $t_1$  in detector  $D_+$ , the state evolves according to Eq.(40), and we find that the normalized state after the detector click is

$$\begin{aligned} |\psi(t_1 + dt)\rangle &= \frac{1}{\sqrt{2}} (b_1^\dagger + b_2^\dagger) |0, 0\rangle, \\ &= \frac{1}{\sqrt{2}} (|1, 0\rangle + |0, 1\rangle). \end{aligned} \quad (43)$$

The probability density for this detector click to occur between times  $t_1$  and  $t_1 + dt$ , conditional on no clicks being observed up to time  $t_1$ , is given by  $p(t_1, +)dt = ||R_+ |\tilde{\psi}(t_1)\rangle||^2 dt = \kappa e^{-2\kappa t_1} dt$ . Note that Eq. (43) implies that the sources become entangled after the first detector click. Furthermore, the state of the system immediately after this first click is independent of both the click time  $t_1$  and the detuning of the two photons,  $\Delta$ .

Conditional on no clicks being observed between times  $t_1 + dt$  and  $t_2$ , the state again evolves under the Schrödinger equation with  $H_{\text{cond}}$ , as

$$\begin{aligned} |\tilde{\psi}(t_2)\rangle &= \exp[-\frac{i}{\hbar} H_{\text{cond}}(t_2 - t_1)] |\psi(t_1 + dt)\rangle, \\ &= \frac{1}{\sqrt{2}} \left( e^{-(i\omega_1 + \frac{\kappa}{2})(t_2 - t_1)} |1, 0\rangle \right. \\ &\quad \left. + e^{-(i\omega_2 + \frac{\kappa}{2})(t_2 - t_1)} |0, 1\rangle \right), \\ &= \frac{e^{-(i\omega_1 + \frac{\kappa}{2})(t_2 - t_1)}}{\sqrt{2}} \left( |1, 0\rangle + e^{i\Delta(t_2 - t_1)} |0, 1\rangle \right). \end{aligned} \quad (44)$$

Note that the relative phase between the two terms in this expression oscillates in time at a rate  $\Delta$ . It is this oscillation that leads to the ‘quantum beats’ in the photon coalescence probability.

A little algebra shows that the probability density for the second detector click to occur in detector  $D_+$ , between times  $t_2$  and  $t_2 + dt$ , conditional on the first click

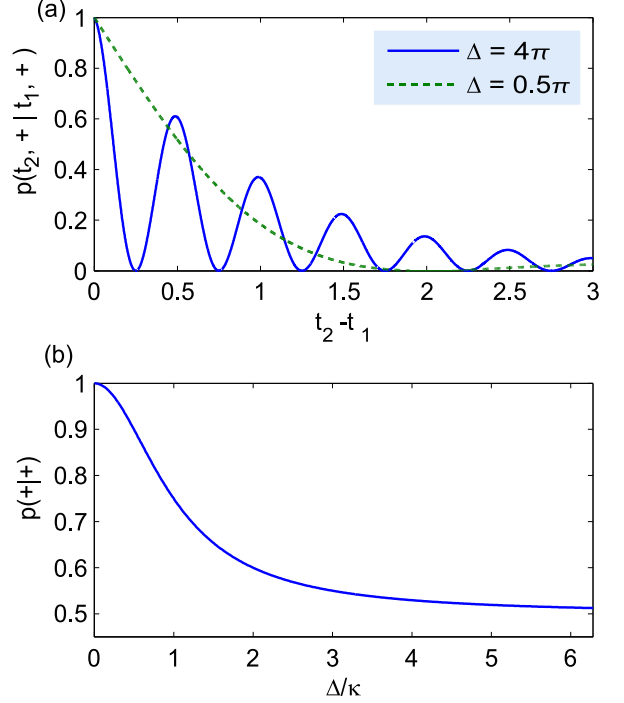


FIG. 7: (Colour online) Generalized Hong-Ou-Mandel effect with detuned photons. (a) Probability density function for observing both clicks in the same detector,  $p(t_2, +|t_1, +) = p(t_2, -|t_1, -)$ , as a function of the delay between clicks,  $(t_2 - t_1)$ . This probability density oscillates at a rate  $\Delta$ , the detuning between the center frequencies of the two photons.  $\kappa = 1$ ,  $\Delta = 4\pi$  (solid curve),  $\Delta = 0.5\pi$  (broken curve). (b) Total coalescence probability,  $p(++)=p(--)$  as a function of detuning,  $\Delta/\kappa$ . This corresponds to the coincidence signal that can be measured if no timing information is available from the detectors.

being observed in  $D_+$  at time  $t_1$ , is given by

$$\begin{aligned} p(t_2, +|t_1, +) &= ||R_+ |\tilde{\psi}(t_2)\rangle||^2, \\ &= \kappa e^{-\kappa(t_2 - t_1)} \cdot \frac{1}{2} \{1 + \cos[\Delta(t_2 - t_1)]\}. \end{aligned} \quad (45)$$

Combining this with the expression for  $p(t_1, +)$  given above we find that the total joint probability distribution for two clicks in detector  $D_+$  is given by  $p(t_1, t_2, +, +) = p(t_2, +|t_1, +)p(t_1, +) = \kappa^2 e^{-\kappa(t_2 + t_1)} \{1 + \cos[\Delta(t_2 - t_1)]\} / 2$ . The somewhat more instructive expression  $p(t_2, +|t_1, +)$  is plotted as a function of  $t_2 - t_1$  in Figure 7 (a).

The central result of this section is that the probability of finding both photons in the same detector oscillates with frequency  $\Delta$ , the detuning of the two photons. This is in agreement with corresponding theoretical and experimental results in Refs. [4] and [5], although we have used a different method to arrive at the result [45].

### B. Bad detector limit

From the results of the previous section, it is straightforward to calculate the total photon coalescence probability - that is, the total probability that both photons will arrive in the same detector. This can also be thought of as the visibility of the Hong-Ou-Mandel effect in the limit of bad photodetectors, i.e. detectors whose time resolution is much longer than the inverse of the detuning,  $\Delta^{-1}$ . We assume that in other respects, the detectors are ideal, in particular that their detection efficiency is unity, and no photons are missed due to dead time. In this limit, the only information available from the detectors is the total number of photons arriving at each detector, and no information about the time of arrival is available.

The total photon coalescence probability,  $p(+|+) = p(-|-)$  for observing both clicks in detector  $D_+$  is given by integrating Eq. (45) over all values of  $\tau = t_2 - t_1$ ,

$$\begin{aligned} p(+|+) &= \int_0^\infty d\tau p(t_2, +|t_1, +), \\ &= \int_0^\infty d\tau \kappa e^{-\kappa\tau} \cdot \frac{1}{2} \{1 + \cos \Delta\tau\}, \\ &= \frac{1}{2} \left( 1 + \frac{\kappa^2}{\kappa^2 + \Delta^2} \right). \end{aligned} \quad (46)$$

This expression is plotted in Figure 7(b). For small detuning,  $\Delta \ll \kappa$ ,  $p(+|+)$  approaches unity, indicating near perfect Hong-Ou-Mandel photon coalescence. For  $\Delta \gg \kappa$ ,  $p(+|+) \simeq 1/2$ , indicating that the photons apparently act as independent particles, scattering randomly into both output ports of the beam splitter.  $\kappa$  can be thought of as the bandwidth of the photons, giving the spread in frequency of each photon about its center value. Thus these results agree with the usual intuition that HOM interference can not be observed between distinguishable photons. However, it is important to note that this is a consequence of the poor time resolution of the detectors. As we saw in the Section IV A, with sufficiently fast time resolved detectors, a modified form of the HOM interference can be observed.

### C. Intermediate detector case

In Sections IV A and IV B we discussed the HOM effect in the limiting cases of perfect time resolution photodetectors, and the limit of bad detectors (with no time resolution), respectively. In general, experiments may be in neither limit, and the detectors may have a finite time resolution which is comparable to the inverse of the detuning between the incident photons. In view of the applications of the HOM effect in quantum information processing, it is useful to have a quantitative understanding of the effect of finite time resolution detectors. In this section, we apply the model of finite time resolution de-

tection introduced in III C to analyse the HOM effect in this regime.

As in Section III C we model the detector by the set of equations

$$\begin{aligned} \dot{\rho}_{RR} &= (\mathcal{L} - J[R_+] - J[R_-])\rho_{RR}, \\ \dot{\rho}_+ &= (\mathcal{L} - J[R_-] - \gamma_r)\rho_+ + J[R_+]\rho_{RR}, \\ \dot{\rho}_- &= (\mathcal{L} - J[R_+] - \gamma_r)\rho_- + J[R_-]\rho_{RR}, \\ \dot{\rho}_{TT} &= (\mathcal{L} - 2\gamma_r)\rho_{TT} + J[R_-]\rho_+ + J[R_+]\rho_-, \end{aligned} \quad (47)$$

where, as before,  $\mathcal{L}\rho \equiv -\frac{i}{\hbar}(H_{\text{cond}}\rho - \rho H_{\text{cond}}^\dagger) + R_+\rho R_+^\dagger + R_-\rho R_-^\dagger$  is the Lindblad master equation,  $J[R]\rho \equiv R\rho R^\dagger$  is the jump matrix, and  $\gamma_r$  is the stochastic decay rate at which a triggered detector will signal a click and return into the ready state. Now, however, the system under observation is that shown in Figure 6, with  $H_{\text{cond}}$  is given by Eq. (39), and the operators  $R_\pm$  are given by Eq. (42). Thus the matrices  $\rho_{RR}$ ,  $\rho_\pm$ ,  $\rho_{TT}$  describe the internal states of the two single mode cavities representing the sources. As in Section IV A, we take the initial state of the system to be the Fock state  $|1, 1\rangle$ , such that  $\rho_{RR}(0) = |1, 1\rangle\langle 1, 1|$ , and  $\rho_\pm(0) = \rho_{TT}(0) = 0$ , indicating that both detectors are in the ‘Ready’ (R) state at time  $t = 0$ .

We are interested in quantities such as  $p_\gamma(t_1, t_2, +, +)$ , which is the probability density function for pairs of *observed* detector clicks. This can be found by first solving Eqs. (47) to find  $\rho_j(t_1)$ . At a given time  $t_1$ , the total probability for detector  $D_+$  to be in the ‘Triggered’ (T) state is  $\text{Tr}[\rho_+(t_1) + \rho_{TT}(t_1)]$ . Thus the probability density for the first  $D_+$  detector click is given by

$$p_\gamma(t_1, +) = \gamma_r \text{Tr}[\rho_+(t_1) + \rho_{TT}(t_1)]. \quad (48)$$

After the first  $D_+$  detector click, the state of the system is updated and renormalized according to

$$\begin{aligned} \rho_{RR}(t_1 + dt) &= \frac{\rho_+(t_1)}{\text{Tr}[\rho_+(t_1) + \rho_{TT}(t_1)]}, \\ \rho_+(t_1 + dt) &= 0, \\ \rho_-(t_1 + dt) &= \frac{\rho_{TT}(t_1)}{\text{Tr}[\rho_+(t_1) + \rho_{TT}(t_1)]}, \\ \rho_{TT}(t_1 + dt) &= 0. \end{aligned} \quad (49)$$

This state is then used as an initial condition to Eqs. 47, which can be solved to give  $\rho_j(t_2|t_1, +)$ , i.e. the state of the system at time  $t_2$ , conditional on a  $D_+$  click at time  $t_1$ , and no clicks between times  $t_1$  and  $t_2$ . The conditional probability density for the second click, in detector  $D_+$ , is then given by

$$p_\gamma(t_2, +|t_1, +) = \gamma_r \text{Tr}[\rho_+(t_2|t_1, +) + \rho_{TT}(t_2|t_1, +)]. \quad (50)$$

The joint probability distribution for  $D_+$  clicks at time  $t_1$  and  $t_2$  can then be formed from Eqs. (48) and (50) as  $p_\gamma(t_1, t_2, +, +) = p_\gamma(t_2, +|t_1, +)p_\gamma(t_1, +)$ . Note that, unlike in the ideal detector case described in Section IV A,  $p_\gamma(t_2, +|t_1, +)$  is no longer just a function of  $t_2 - t_1$ , but in fact depends on the value of  $t_1$ .

In principle, quantities such as  $p_\gamma(t_1, t_2, +, +)$  can be obtained analytically by first finding the general solution of Eqs. (47) and then applying the above steps. However, this turns out to be difficult in general. Unlike the case of the distant-atom entangling scheme presented in Section III B, it is not possible to concentrate on the single photon terms in the expressions for  $\rho_j$ . Instead, all terms must be tracked, including in particular those which correspond to both photons entering the same detector within a short interval. This means that all 64 coupled equations in Eqs. (47) must be solved. Owing to this complexity, we resort to a numerical solution of Eqs. (47), using the MATLAB ‘ode45’ function. Following the steps outlined above, we obtain  $p_\gamma(t_1, t_2, +, +)$ . From this quantity, we can determine  $p_\gamma(\tau, +|+)$ , that is, the distribution of intervals  $\tau = t_2 - t_1$  between detector clicks, given that the first click was observed in detector  $D_+$ . This is the analogous quantity to  $p(t_2, +|t_1, +)$ , in the case of ideal detectors, which was plotted in Figure 7 (a).  $p_\gamma(\tau, +|+)$  is given by

$$p_\gamma(\tau, +|+) = \frac{\int_0^\infty dt_1 p_\gamma(t_1, t_1 + \tau, +, +)}{\int_0^\infty dt_1 p_\gamma(t_1, +)} \quad (51)$$

We can also calculate  $p_\gamma(\tau, -|+)$ , which is the probability distribution for the second click to occur in  $D_-$ , given that the first was in  $D_+$ , in a similar way. In practice, we set the upper limit of the integrals to a value of  $3\kappa^{-1}$ , which leads to a slight relative underestimate of approximately  $\exp[-2\kappa \times 3\kappa^{-1}] \approx 0.25\%$  in the value of these integrals.  $p_\gamma(\tau, +|+)$  is plotted in Figure 8(a), along with the ideal result,  $p(t_2, +|t_1, +)$  from Eq. (45), for the same values of  $\Delta$  and  $\kappa$ . For smaller values of the detector response rate,  $\gamma_r$ , it can be seen that the interference fringes become washed out. This reduction in visibility is a result of the finite time response of the detectors. More specifically, as  $\gamma_r$  approaches  $\Delta$  it becomes harder to resolve the individual interference fringes.

A reasonable figure of merit for this generalized HOM effect is the fringe visibility,

$$v(\tau) = \left| \frac{p_\gamma(\tau, +|+) - p_\gamma(\tau, -|+)}{p_\gamma(\tau, +|+) + p_\gamma(\tau, -|+)} \right| \quad (52)$$

After an initial transient behaviour on short timescales  $\tau \sim \gamma_r^{-1}$ ,  $v(\tau)$  is, to a good approximation, a periodic function, with maxima at integer multiples of  $\pi/\Delta$ . A good figure of merit is therefore the value of these maxima (taken outside the initial transient region). In Figure 8(b) we plot the fringe visibility evaluated at  $\tau = 20 \times \pi/\Delta$ , as a function of detector response rate,  $\gamma_r$ , for a particular choice of  $\Delta$  and  $\kappa$ . As expected, the fringe visibility vanishes for slow detectors, and approaches unity for fast detectors with  $\gamma_r \gg \Delta$ .

## V. OUTLOOK AND CONCLUSIONS

In this paper we have looked at the effect of frequency mismatch in two schemes which make use of few-photon

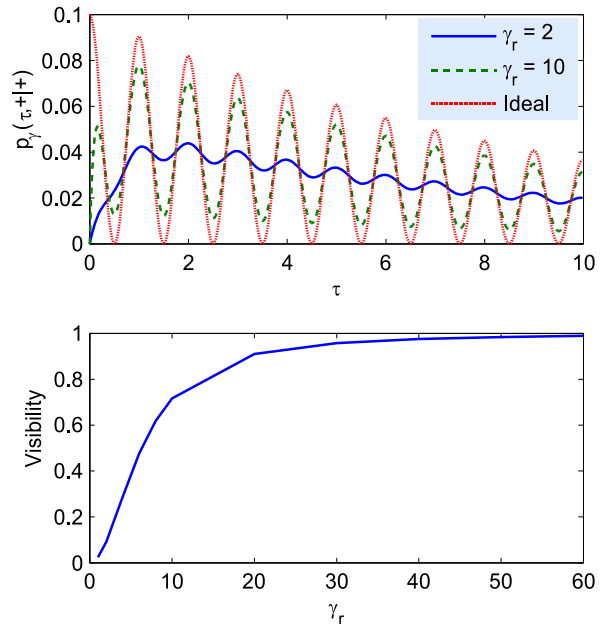


FIG. 8: (Colour online) Generalized Hong-Ou-Mandel effect with detuned photons and finite time response detectors. (a) Probability density function for observing both clicks in the same detector,  $p_\gamma(\tau, +|+)$ , as a function of the delay between clicks,  $\tau = t_2 - t_1$ .  $\kappa = 0.1$ ,  $\Delta = 2\pi$ ,  $\gamma_r = 2$  (solid curve),  $\gamma_r = 10$  (broken curve). The dotted curve shows the result corresponding to ideal detectors, i.e.  $p(t_2, +|t_1, +)$  from Eq. (45), for the same values of  $\kappa$  and  $\Delta$ . (b) Fringe visibility at  $\tau = 20 \times \pi/\Delta$  as a function of detector response rate,  $\gamma_r$ , for the same  $\kappa$  and  $\Delta$  as in (a).

interference. Our main conclusions can be summarized as follows.

We first looked at the effect of frequency mismatch in the distributed QIP scheme of Barrett and Kok [1]. One key finding was that, with idealized detectors (i.e. such that the detector response rate  $\gamma_r$  is much faster than the photon detuning  $\Delta$ ) perfect entanglement of distant atoms is still possible. The entangled states pick up a known phase that depends on the times of the photodetection events, and which can be corrected via a local unitary operation. This is true as long as the cavity mismatch is known from, e.g. previous measurements on the cavities. Any unknown variations in this parameter cannot be rectified. In the opposite limit of poor time resolution detectors ( $\gamma_r \ll \Delta$ ) the fidelity of the resulting mixed entangled state depends on the overlap of the photons’ spectra according to Eq. (28).

With the aid of a model of the internal dynamics of the photodetector, we were also able to analyse the intermediate case, where the detector response rate,  $\gamma_r$  is of similar order to  $\Delta$ . Here, we found that as  $\gamma_r$  exceeds  $\Delta$ , the fidelity of the entangled states approaches unity. The numerical results suggest that the error in the entangling operation (that is,  $1 - \bar{F}$ , with  $\bar{F}$  the average

fidelity of Eq. (38)) scales approximately quadratically with  $\Delta/\gamma_r$ , such that an error of  $1 - \bar{F} \sim 10^{-4}$  is possible with  $\Delta/\gamma_r \sim 10^{-2}$ .

We also analysed the Hong-Ou-Mandel effect with detuned photons, and arrived at similar conclusions. In the case of idealized detectors with time resolution much larger than the photon detuning, a modified Hong-Ou-Mandel effect can be observed, with the coalescence probability oscillating as a function of time, at angular frequency given by  $\Delta$ , the detuning of the two sources. This result is in agreement with earlier theoretical and experimental results by Legero *et al.* [4, 5], although our approach was slightly different to this earlier work. We also extended the analysis to the case of non-ideal detectors, and found that the fringe visibility of this modified Hong-Ou-Mandel effect decreases dramatically as  $\gamma_r$  is reduced below  $\Delta$ , but approaches unity for  $\gamma_r \gg \Delta$ .

The usual understanding of few-photon interference effects is that they can only be observed with identical photons. This is because experiments such as those considered here make use of a beam splitter to coherently erase ‘which path’ information. Thus any ‘excess’ information, such as frequency or polarization, carried by the photon, that can be used, even if only in principle, to infer the previous path of the photon, will typically degrade the interference effect. Even if the detector has no output corresponding to the energy of the incident photon, we could imagine that this information might be encoded in the internal state of the detector, e.g. in the energy of the exciton-hole pair created when the photon was initially absorbed, and so it could be determined, in principle, with a careful measurement of the microscopic state of the detector.

This is in apparent contradiction with the results of this paper, which predict that a modified version of such interference effects can be observed with high fidelity even when the photons are spectrally distinct. How can the results here be reconciled with the conventional understanding described in the previous paragraph? One way of understanding this is that detectors with sufficiently good time resolution are themselves capable of erasing some of this ‘excess’ frequency information. Loosely speaking, for a detector with time resolution  $\gamma_r^{-1}$ , a detected photon is localized in a time window of corresponding duration  $\gamma_r^{-1}$ . Thus the frequency uncertainty of the detected photon *must* be equal to or larger than  $\gamma_r$ . This means that there is no way, even in principle, of determining the frequency of the detected photon. Thus the ‘excess’ frequency information has been successfully

erased.

Our results should also shed light on the question of where the interference ‘goes’ in few photon interference experiments with detuned photons. With idealized detectors with high temporal resolution, we have seen that a modified version of the interference or entanglement is present, and in this sense there is no loss of interference visibility or entanglement. With imperfect detectors, the corresponding effects are diminished. Therefore another way of understanding these results is to say that imperfect detectors introduce noise into the interference pattern, because the timing of the detector clicks produces additional randomness above what would be expected from spontaneous emission alone.

We conclude by suggesting some possibilities for future work on the subject of few photon interference with detuned photons. One immediate application of our work is that it can be used to place design constraints on near future experiments - given detectors with a particular temporal resolution (as quantified by  $\gamma_r$  in this work), we know that the sources must be tuned such that  $\Delta \lesssim \gamma_r$  in order to see the corresponding interference or entanglement effect with reasonable visibility/fidelity. Conversely, if tuning the sources is difficult, we know the corresponding detector resolution required.

Similarly, for scalable quantum computation, the results here can be used to place constraints that the physical parameters  $\Delta$  and  $\gamma_r$  must satisfy in order to implement a fault-tolerant computation scheme, either in a hybrid matter-light setup [1], or in a linear optical scheme [2, 3, 43]. In this case, some further work is required in order to relate the physical errors due to frequency mismatch and finite detector response rate to the more abstract error models employed in the analysis of fault tolerant computation schemes.

Finally, although we have concentrated on two particular examples of few photon interference in this paper, the results presented here, the methods used to arrive at them, and the resulting physical insights, should carry over to many other few photon interference setups. We therefore hope these results have useful implications for quantum information processing schemes which utilize few photon interference.

*Acknowledgments:* We thank Jeremy O’Brien, Andrew Doherty, Peter Knight and in particular Tom Stace for a number of stimulating and encouraging conversations. SDB was supported by the EPSRC. JM was supported by the EPSRC through the Quantum Information Processing IRC.

---

[1] S. D. Barrett and P. Kok, Phys. Rev. A **71**, 060310 (2005).  
 [2] E. Knill, R. Laflamme, and G. J. Milburn, Nature **409**, 46 (2001).  
 [3] P. Kok, W. J. Munro, K. Nemoto, T. C. Ralph, J. P. Dowling, and G. J. Milburn, Rev. Mod. Phys. **79**, 135

(2007).  
 [4] T. Legero, T. Wilk, A. Kuhn, and G. Rempe, Applied Physics B **77**, 797 (2003).  
 [5] T. Legero, T. Wilk, M. Hennrich, G. Rempe, and A. Kuhn, Phys. Rev. Lett. **93**, 070503 (2004).  
 [6] C. K. Hong, Z. Y. Ou, and L. Mandel, Phys. Rev. Lett.

- 59**, 2044 (1987).
- [7] C. Cabrillo, J. I. Cirac, P. Garcia-Fernandez, and P. Zoller, *Phys. Rev. A* **59**, 1025 (1999).
- [8] S. Bose, P. Knight, M. Plenio, and V. Vedral, *Phys. Rev. Lett.* **83**, 5158 (1999).
- [9] N. Yoran and B. Reznik, *Phys. Rev. Lett.* **91**, 037903 (2003).
- [10] M. A. Nielsen, *Phys. Rev. Lett.* **93**, 040503 (2004).
- [11] D. E. Browne and T. Rudolph, *Phys. Rev. Lett.* **95**, 010501 (2005).
- [12] Y. L. Lim, A. Beige, and L. C. Kwek, *Phys. Rev. Lett.* **95**, 030505 (2005).
- [13] Y. L. Lim, S. D. Barrett, A. Beige, P. Kok, and L. C. Kwek, *Phys. Rev. A* **73**, 012304 (2006).
- [14] L.-M. Duan, M. J. Madsen, D. L. Moehring, P. Maunz, R. N. Kohn, and C. Monroe, *Phys. Rev. A* **73**, 062324 (2006).
- [15] D. L. Moehring, P. Maunz, S. Olmschenk, K. C. Younge, D. N. Matsukevich, L.-M. Duan, and C. Monroe, *Nature* **449**, 68 (2007).
- [16] J. Beugnon, M. P. A. Jones, J. Dingjan, B. Darqui, G. Messin, A. Browaeys, and P. Grangier, *Nature* **440**, 779 (2006).
- [17] L.-M. Duan, M. Lukin, J. I. Cirac, and P. Zoller, *Nature* **414**, 413 (2001).
- [18] Z.-B. Chen, Y.-A. C. Bo Zhao, J. Schmiedmayer, and J.-W. Pan, [quant-ph/0609151](https://arxiv.org/abs/quant-ph/0609151) (????).
- [19] C.-W. Chou, J. Laurat, H. Deng, K. S. Choi, H. de Riedmatten, D. Felinto, and H. J. Kimble, *Science* **316**, 1316 (2007).
- [20] K. Vahala, *Nature* **424**, 839 (2003).
- [21] P. Tamarat, T. Gaebel, J. R. Rabeau, M. Khan, A. D. Greentree, H. Wilson, L. C. L. Hollenberg, S. Praver, P. Hemmer, F. Jelezko, et al., *Phys. Rev. Lett.* **97**, 083002 (2006).
- [22] P. Warszawski, H. M. Wiseman, and H. Mabuchi, *Phys. Rev. A* **65**, 023802 (2002).
- [23] P. Warszawski and H. M. Wiseman, *J. Opt. B.* **5**, 1 (2003).
- [24] T. M. Stace, G. J. Milburn, and C. H. Barnes, *Phys. Rev. B* **67**, 085317 (2003).
- [25] N. S. Jones and T. M. Stace, *Phys. Rev. B* **73**, 033813 (2006).
- [26] D. E. Browne, M. B. Plenio, and S. F. Huelga, *Phys. Rev. Lett.* **91**, 067901 (2003).
- [27] X.-L. Feng, Z.-M. Zhang, X.-D. Li, S.-Q. Gong, and Z.-Z. Xu, *Phys. Rev. Lett.* **90**, 217902 (2003).
- [28] L.-M. Duan and H. J. Kimble, *Phys. Rev. Lett.* **90**, 253601 (2003).
- [29] C. Simon and W. T. M. Irvine, *Phys. Rev. Lett.* **91**, 110405 (2003).
- [30] I. E. Protsenko, G. Reymond, N. Schlosser, and P. Grangier, *Phys. Rev. A* **66**, 062306 (2002).
- [31] X. Zou and W. Mathis, *Phys. Rev. A* **71**, 042334 (2005).
- [32] H.-A. Engel, J. M. Taylor, M. D. Lukin, and A. Imamoglu, [cond-mat/0612700](https://arxiv.org/abs/cond-mat/0612700) (2006).
- [33] P. Rohde and S. D. Barrett, *New J. Phys.* **9**, 198 (2007).
- [34] H. Carmichael, *An Open Systems Approach to Quantum Optics* (Springer-Verlag, 1993).
- [35] H.-P. Breuer and F. Petruccione, *The Theory of Open Quantum Systems* (Oxford University Press, 2002).
- [36] A. Beige, Ph.D. thesis, Georg-August-Universität zu Göttingen (1997).
- [37] G. C. Hegerfeldt and D. G. Sondermann, *Quantum and Semiclassical Optics: Journal of the European Optical Society Part B* **8**, 121 (1996).
- [38] M. B. Plenio and P. L. Knight, *Rev. Mod. Phys.* **70**, 101 (1998).
- [39] J. Metz and A. Beige, *Phys. Rev. A* **76**, 022331 (2007).
- [40] C. Santori, D. Fattal, J. Vuckovic, G. S. Solomon, and Y. Yamamoto, *Nature* **419**, 594 (2002).
- [41] J. Beugnon, M. P. A. Jones, J. Dingjan, B. Darqui, G. Messin, A. Browaeys, and P. Grangier, *Nature* **440**, 779 (2006).
- [42] P. Maunz, D. L. Moehring, M. J. Madsen, J. R. N. Kohn, K. C. Younge, and C. Monroe, [quant-ph/0608047](https://arxiv.org/abs/quant-ph/0608047) (????).
- [43] D. E. Browne and T. Rudolph, *Phys. Rev. Lett.* **95**, 010501 (2005).
- [44] Note that, in general, the scheme can be applied to a variety of different qubit realizations such as trapped atoms, ions, quantum dots, or impurity centers in solids, provided they have the appropriate level structure of Figure 1 (a). Hereafter, we shall just refer to the systems as ‘atoms’ for brevity.
- [45] Note that our expressions for the time resolved photon coalescence probability density differ slightly from those considered in Ref. [4]. The differences are due to the fact that we consider exponentially decaying photon temporal wavefunctions, arising from a sudden excitation of the source at time  $t = 0$  followed by spontaneous emission, whereas Ref. [4] considers Gaussian temporal wavefunctions.